

G Protein $\beta\gamma$ Subunits and AGS3 Control Spindle Orientation and Asymmetric Cell Fate of Cerebral Cortical Progenitors

Kamon Sanada¹ and Li-Huei Tsai^{1,2,*}

¹Department of Pathology

²Howard Hughes Medical Institute

Harvard Medical School

77 Avenue Louis Pasteur

Boston, Massachusetts 02115

Summary

Neurons in the developing mammalian brain are generated from progenitor cells in the proliferative ventricular zone, and control of progenitor division is essential to produce the correct number of neurons during neurogenesis. Here we establish that G $\beta\gamma$ subunits of heterotrimeric G proteins are required for proper mitotic-spindle orientation of neural progenitors in the developing neocortex. Interfering with G $\beta\gamma$ function in progenitors causes a shift in spindle orientation from apical-basal divisions to planar divisions. This results in hyperdifferentiation of progenitors into neurons as a consequence of both daughter cells adopting a neural fate instead of the normal asymmetric cell fates. Silencing AGS3, a nonreceptor activator of G $\beta\gamma$, results in defects similar to the impairment of G $\beta\gamma$, providing evidence that AGS3-G $\beta\gamma$ signaling in progenitors regulates apical-basal division and asymmetric cell-fate decisions. Furthermore, our observations indicate that the cell-fate decision of daughter cells is coupled to mitotic-spindle orientation in progenitors.

Introduction

In the developing mammalian neocortex, projection neurons are primarily generated from neural progenitor cells that occupy the proliferative ventricular zone (VZ) of the cerebral wall. Newborn neurons then migrate away from their birthplace toward the cortical surface and form cortical layers. It is widely accepted that radial glial cells serve as neural progenitor cells (Noctor et al., 2001) and can generate neurons over multiple divisions at different times during corticogenesis.

Progenitor cells in the mammalian cerebral cortex likely undergo both symmetric and asymmetric cell divisions. Prior to the onset of neurogenesis, most progenitor cells undergo symmetric cell division to produce two daughters that both adopt the progenitor fate. This symmetric division expands the pool of progenitor cells that will ultimately give rise to neurons in the nervous system. As cortical development proceeds, progenitor cells begin to undergo asymmetric cell division. This asymmetric division produces two distinct daughter cells, with one differentiating into a neuron and the other remaining a progenitor cell (Chenn and McConnell, 1995; Takahashi et al., 1996; Miyata et al., 2001; Noctor et al., 2001). Toward the end of cortico-

genesis, progenitors revert back to symmetric cell division, giving rise to two daughters that both differentiate into neurons (Kornack and Rakic, 1995; Takahashi et al., 1996; Miyata et al., 2001; Cai et al., 2002). Interestingly, the progenitor cleavage plane changes over the course of corticogenesis (Chenn and McConnell, 1995; Haydar et al., 2003). Progenitors in the early stage of corticogenesis (embryonic day 10–12 in mice) divide with the cleavage plane perpendicular to the ventricular surface (vertical cleavage plane). However, the frequency of progenitors dividing with the cleavage plane parallel to the ventricular surface (horizontal cleavage plane) increases (Chenn and McConnell, 1995; Haydar et al., 2003) as development proceeds, peaking at E14–15 in mice. At later stages of neurogenesis, most progenitor cells reorient their cleavage plane back to the vertical axis (Haydar et al., 2003). Thus, the orientation of the mitotic spindle of progenitors correlates with the cell-fate decision of the two daughter cells. However, to date, there is no evidence demonstrating that manipulation of mitotic-spindle orientation can alter the fate of daughter cells. In addition, the molecular mechanism by which spindle orientation is regulated remains unsolved.

Recent studies in *Drosophila* and *C. elegans* have shown that heterotrimeric guanine-nucleotide binding regulatory proteins (G proteins) participate in asymmetric cell division by regulating spindle positioning and orientation (reviewed in Betschinger and Knoblich, 2004). Heterotrimeric G proteins are composed of α , β , and γ subunits and are classified based on the primary sequences of G α subunits into four main families: G α_s , G α_i , G α_q , and G α_{12} . Classically, G proteins are coupled to G protein-coupled receptors (GPCRs), and receptor stimulation induces the exchange of GDP by GTP on the G α subunit, resulting in the dissociation of the heterotrimer into GTP bound G α and free G $\beta\gamma$. Both the GTP bound G α and dissociated G $\beta\gamma$ then function as active signaling modules that regulate various downstream effectors (reviewed in Gilman, 1987). Importantly, in *Drosophila* neuroblasts and *C. elegans* embryos, the G α_i and G $\beta\gamma$ subunits are associated with asymmetric cell division. Moreover, it is suggested that their activation is unlikely to be mediated by GPCRs but rather by the nonreceptor activators, GPR-1/2 in *C. elegans* and Partner of Inscuteable (Pins) in *Drosophila* (Schaefer et al., 2001; Gotta et al., 2003). These activators are orthologs of mammalian AGS3 (activator of G protein signaling 3), originally identified as one of the receptor-independent activators of G $\beta\gamma$ signaling (Cismowski et al., 1999; Takesono et al., 1999), and mammalian Pins (Mochizuki et al., 1996). In the developing mammalian brain, G α_{i2} is selectively expressed in the VZ (Asano et al., 2001), and inhibition of Gi protein signaling by pertussis toxin results in the reduction of proliferating cells in the neocortex (Shinohara et al., 2004). This result raises the possibility that G α_i /G $\beta\gamma$ plays a role in the proliferation of neural progenitors.

In the present study, we show that the G $\beta\gamma$ subunits

*Correspondence: li-huei_tsai@hms.harvard.edu

of heterotrimeric G proteins play a key role in orienting the mitotic spindle perpendicular to the ventricular surface (along the apical-basal axis) in the developing neocortex. We also demonstrate that shifting the mitotic spindle from the apical-basal to planar axis by disrupting the G $\beta\gamma$ signaling is associated with hyperdifferentiation of progenitors and overproduction of neurons. In addition, we provide evidence that G $\beta\gamma$ is required for asymmetric cell-fate choices of progenitors. These findings suggest that the spindle orientation of progenitor cells is coupled to daughter cell-fate choices in the developing neocortex. Furthermore, our results indicate that AGS3 functions as an activator of G $\beta\gamma$ signaling in cortical progenitors. Together with the polarized distribution of G $\beta\gamma$ in the progenitor cells, this study establishes a link between AGS3-G $\beta\gamma$ signaling and proper spindle orientation, hence asymmetric cell-fate determination of cerebral cortical progenitor cells during mammalian neurogenesis.

Results

G $\beta\gamma$ Signaling Regulates Spindle Orientation of Cortical Progenitor Cells

To determine the progenitor cleavage plane in the developing mouse neocortex, we focused on progenitor cells in anaphase or telophase, as cortical progenitor cells in living E15 brain slices displayed dynamic rotation of the metaphase plate prior to chromosome separation (Figure 1A; see also Movie S1 in the Supplemental Data available with this article online; Haydar et al., 2003). Chenn and McConnell (1995) previously described three alternative orientations of cleavage planes in relation to the ventricular surface, including vertical (60°–90°), intermediate (30°–60°), and horizontal (0°–30°) (Figure 1B). Vertical cleavage is correlated with symmetric, whereas horizontal cleavage is correlated with asymmetric cell division of progenitor cells. When we introduced the GFP-expressing plasmid (pCA-IRES-GFP) into the VZ of E14 embryos by in utero electroporation and analyzed the orientation of cell divisions at E15, GFP-labeled cells displayed various angles of the cleavage plane (Figure 1C) in the lateral aspect of the anterior neocortex where the plasmid was introduced (data not shown). Based on the alignment of chromosomes, approximately 50% of GFP-labeled dividing cells displayed the vertical cleavage plane, 30% the intermediate plane, and the remaining 20% the horizontal cleavage plane (Figures 1D and 1E). Similar distribution of the three alternative division planes was observed in untransfected dividing cells (Figure 1E), suggesting that electroporation or GFP expression per se had no effect on the cleavage plane of cortical progenitor cells.

To determine whether G proteins are involved in this process, we took advantage of the finding that overexpression of the carboxy-terminal region of β -adrenergic receptor kinase (β ARK-ct) blocks G $\beta\gamma$ -dependent signaling events by sequestering free G $\beta\gamma$ without affecting G α signaling (Koch et al., 1994). When β ARK-ct-expressing plasmid (pCA- β ARK-ct-IRES-GFP) was introduced into the VZ, a larger population (approximately 72%) of cells divided with the vertical cleavage plane, and only 28% displayed either the intermediate or the horizontal cleav-

age plane (Figure 1E). The significant effect of β ARK-ct on altering the cleavage plane suggests that active G $\beta\gamma$ contributes to proper mitotic-spindle orientation in cortical progenitor cells. To further verify the role of G $\beta\gamma$ signaling, we expressed wild-type G α i, which is known to sequester free G $\beta\gamma$ and thereby inhibit G $\beta\gamma$ signaling (Federman et al., 1992; Crespo et al., 1994). Similar to the overexpression of β ARK-ct, overexpression of G α i3 altered the orientation of the cleavage plane (Figures 1D and 1E). To exclude the possibility that the alteration of the cleavage plane observed upon overexpression of wild-type G α i is due to spontaneous GDP-GTP exchange and activation of introduced G α i, we transfected G α i3(Q204L), a GTPase-deficient constitutively active form of G α i3. Expression of G α i3(Q204L) had no effect on spindle orientation (Figure 1E), suggesting that the alteration of spindle orientation induced by overexpression of G α i3 is due to the sequestration of G $\beta\gamma$.

We also examined the mitotic spindles using an α -tubulin antibody. As shown in Figures 1F and 1G, the relative frequencies of vertical, intermediate, and horizontal cleavage planes after overexpression of β ARK-ct were similar to those analyzed according to the chromosome orientation (Figures 1D and 1E). β ARK-ct expression did not seem to affect the microtubule network. Taken together, these observations suggest that G $\beta\gamma$ signaling controls the spindle orientation of dividing progenitor cells and participates in progenitor division along the apical-basal axis in the developing neocortex.

Impaired G $\beta\gamma$ Signaling Promotes Neurogenesis in the Neocortex

The altered orientation of cleavage planes in G $\beta\gamma$ -impaired progenitors suggests that potential changes in cell fate might occur in the daughter cells. To test this hypothesis, we electroporated embryonic brains at E13 and analyzed the identities of GFP-labeled cells at E14 (Figure 2A) using neuronal (Tuj1) and progenitor (Nestin) markers after the cortical cells were dispersed. When the control GFP-expressing plasmid was introduced, approximately 20% of GFP-labeled cells were Tuj1 positive (differentiated neurons), and 80% of GFP-labeled cells remained Nestin-positive progenitors (Figures 2B and 2C). By contrast, when β ARK-ct or G α i3 was introduced, GFP and Tuj1 double-positive cells increased to approximately 50%, which was accompanied by a significant reduction of Nestin-positive progenitors. Thus, these results suggest an important role for G $\beta\gamma$ in regulating neurogenesis in the developing neocortex.

Neuronal Differentiation Is Promoted by Impairment of G $\beta\gamma$ Signaling in Progenitors

To assess whether increased neuron production induced by impaired G $\beta\gamma$ is due to hyperdifferentiation of neural progenitor cells, we examined a potential reduction of the mitotic-cell fraction in β ARK-ct/G α i3-transfected progenitors by immunohistochemistry using the phosphohistone H3 (P-H3) antibody, a marker for mitotic cells. Twenty-four hours after electroporation of the control GFP construct, the majority of GFP-positive cells were located in the VZ, and P-H3-positive cells were arrayed along the ventricular surface where pro-

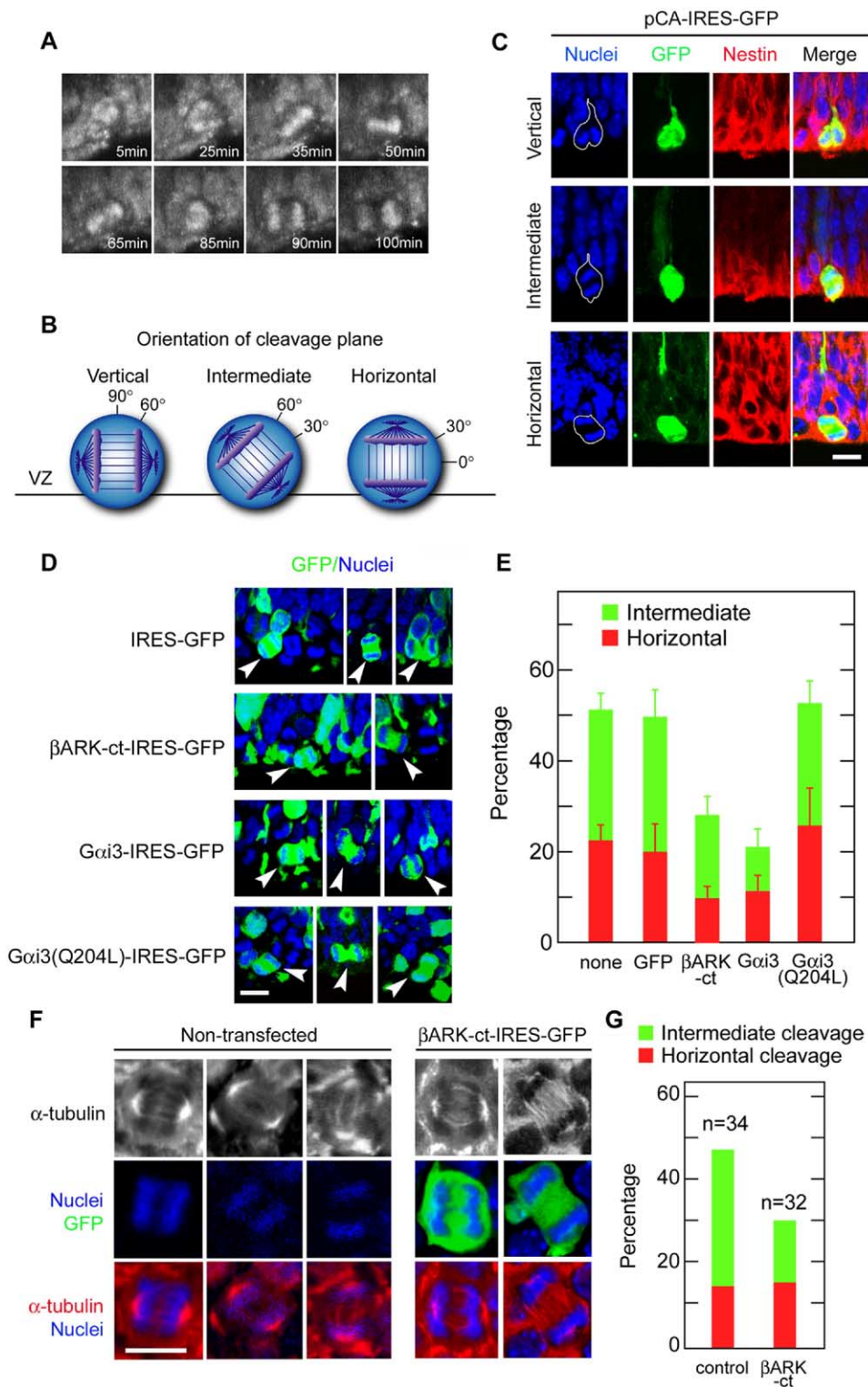


Figure 1. Impairment of G $\beta\gamma$ Signaling Results in an Increase in Progenitor-Cell Division along the Planar Axis

(A) Time-lapse video sequences represent the typical mode of cell division in the VZ of E15 cortical slices labeled with a vital nucleic-acid binding dye, Syto-11. Metaphase plate rotates prior to cleavage (35–65 min). Time is denoted in the bottom right corner.

(B) Dividing progenitor cells are classified into three groups according to the orientation of cleavage plane to the ventricular surface: vertical (60°–90°), intermediate (30°–60°), and horizontal (0°–30°). Cells with vertical and horizontal cleavage have the mitotic spindle parallel to and perpendicular to the VZ, respectively.

(C) pCA-IRES-GFP plasmid was introduced into embryos at E14, and brains were fixed at E15. Brain sections were then stained with antibody-

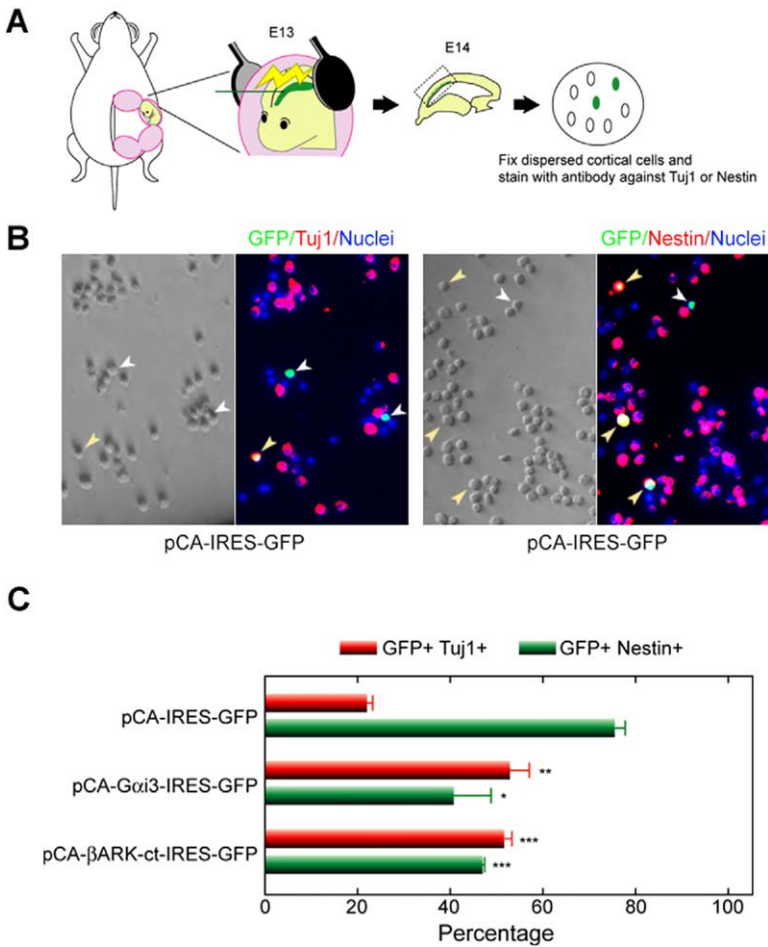


Figure 2. Impaired $G\beta\gamma$ Signaling Induces Overproduction of Neurons

(A) The diagram illustrates the procedure for examining identities of electroporated cerebral cortical cells. Plasmids encoding GFP together with various genes were introduced into embryos at E13. Twenty-four hours later, the anterior neocortex was dissected out and dispersed, followed by fixation and staining of cells with either anti-GFP/Tuj1 antibodies or anti-GFP/Nestin antibodies.

(B) Examples of cortical cells electroporated with the pCA-IRES-GFP plasmid. Images derived from double staining with either anti-GFP/Tuj1 antibodies (left panel) or anti-GFP/Nestin antibodies (right panel) are shown. Phase-contrast images are also shown. Yellow arrowheads represent double-positive cells. White arrowheads represent GFP-positive but Tuj1/Nestin-negative cells.

(C) Percentage of neurons (GFP+ and Tuj1+) to total GFP+ cells and percentage of progenitors (GFP+ and Nestin+) to total GFP+ cells were quantified and plotted as the mean \pm SEM ($n = 3-4$), with the introduced plasmid indicated. * $p < 0.05$, ** $p < 0.01$, *** $p < 0.001$ (one-way ANOVA).

genitor cells undergo mitosis in E15 embryos (Figure 3A). Under this condition, $4.9\% \pm 1.6\%$ ($n = 5$ embryos) of GFP-labeled cells were positive for P-H3 (72 P-H3- and GFP-positive cells/1475 GFP-positive cells located in the VZ) (Figures 3A and 3C). However, when $G\alpha i3$ -expressing plasmid was introduced, only $2.0\% \pm 0.4\%$ ($n = 4$ embryos) of GFP-labeled cells were positive for P-H3 (9 P-H3- and GFP-positive cells/528 GFP-positive cells located in the VZ). A similar significant reduction of the mitotic-cell population was observed in β ARK-ct-transfected cells ($2.6\% \pm 0.2\%$, $n = 3$ embryos, 13 P-H3- and GFP-positive cells/480 GFP-positive cells located in the VZ) (Figures 3A and 3C).

We next sought to determine whether the decrease in mitotic cells in $G\beta\gamma$ -impaired progenitors is due to

the promoted cell-cycle exit of dividing progenitor cells. To this end, embryos were electroporated with the GFP construct at E13, pulse labeled by BrdU at E14, and analyzed at E15 by immunostaining with antibodies to GFP, BrdU, and Ki67 (a marker for cells in the S, G2, and M phases). As indicated by the arrowheads in Figure 3B, GFP-, BrdU-, and Ki67-positive cells represent electroporated cells that were in S phase at E14 and remained in the cell cycle at E15. In contrast, GFP-positive, BrdU-positive, and Ki67-negative cells (arrows in Figure 3B) represent electroporated cells that were in S phase at E14 and exited the cell cycle at E15. We estimated the cell-cycle-exit index of GFP-labeled cells as the ratio of GFP+/BrdU+/Ki67- cells to GFP+/BrdU+ cells (Chenn and Walsh, 2002). When either the $G\alpha i3$ or

ies against GFP (green) and the progenitor marker Nestin (red). Nuclei were stained with Hoechst 33258 (blue). Representative images of dividing progenitor cells with horizontal, intermediate, and vertical cleavage planes near the ventricular surface are shown. GFP-positive cells are outlined with solid lines in the first panels. The ventricular (apical) surface is pointing downward.

(D-G) Plasmids encoding GFP together with various genes were introduced into E14 brains, and brains were fixed at E15.

(D) Representative images of GFP-labeled dividing cells (arrowheads) are shown, with the introduced plasmid indicated.

(E) Relative frequencies of cell divisions with vertical, intermediate (green), and horizontal (red) cleavage planes were measured and plotted as the mean \pm SEM ($n = 3-5$).

(F) Brain sections were stained with antibodies against GFP (green) and α -tubulin (red). Representative images of nontransfected control dividing cells and β ARK-ct/GFP-transfected cells are shown.

(G) The relative frequencies of vertical, intermediate (green), and horizontal (red) cleavage planes were measured and plotted according to the mitotic-spindle orientation (see [B]). Scale bars, 10 μ m.

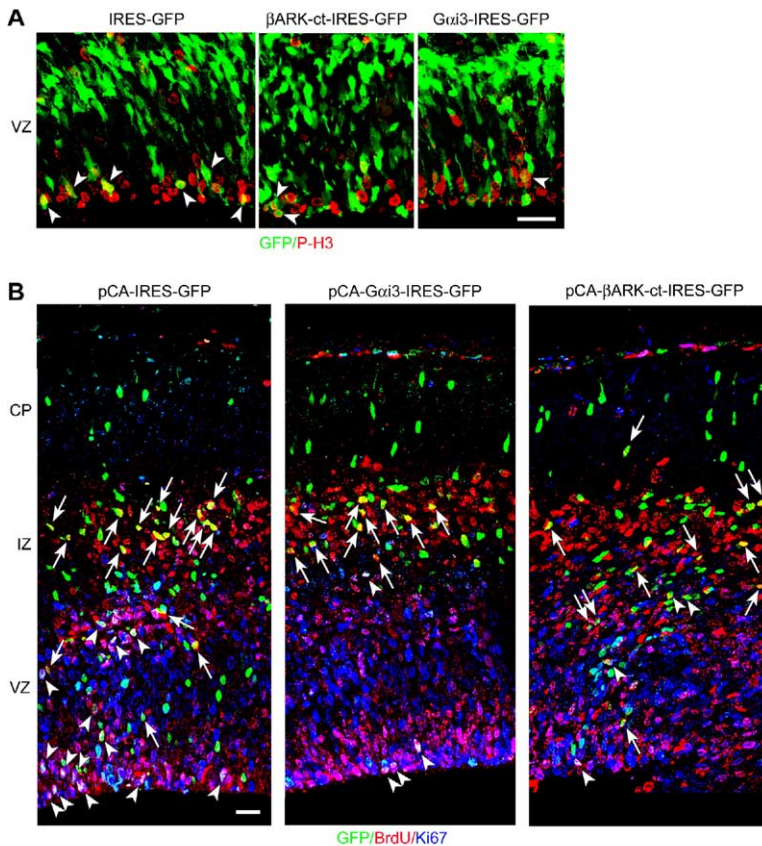


Figure 3. Neural Differentiation of Progenitor Cells Is Promoted by Disruption of $G\beta\gamma$ Signaling

(A) pCA-IRES-GFP (left), pCA- β ARK-ct-IRES-GFP (middle), or pCA- $G\alpha i3$ -IRES-GFP (right) plasmid was electroporated into embryos at E14, and brains were fixed at E15. Brain sections were then stained with antibodies against GFP (green) and the mitotic marker phosphohistone H3 (P-H3, red).

(B) pCA-IRES-GFP (left), pCA- $G\alpha i3$ -IRES-GFP (middle), or β ARK-ct-IRES-GFP (right) plasmid was introduced into embryonic brains at E13; BrdU was administrated at E14; and brains were fixed 24 hr after the BrdU pulse labeling. Brain sections were then stained with antibodies against BrdU (red), the cell-cycle marker Ki67 (blue), and GFP (green). GFP-positive cells labeled with both BrdU and Ki67 (white; arrowheads) remain active in the cell cycle. GFP-positive cells labeled with BrdU but not Ki67 (yellow; arrows) are those that exited the cell cycle.

(C) Mitotic index.
(D) Cell-cycle-exit index. Data are presented as the mean \pm SEM ($n = 3$). * $p < 0.05$, ** $p < 0.01$ (one-way ANOVA). Scale bars, 20 μ m.

β ARK-ct construct was introduced, there was a 2-fold increase in the fraction of GFP-labeled cells that exited the cell cycle compared to when the control plasmid was introduced ($p < 0.01$, ANOVA; Figures 3B and 3D). Consistent with this result, more GFP-labeled cells were located in the intermediate zone and cortical plate of $G\alpha i3$ - or β ARK-ct-electroporated brains compared to control plasmid-expressing brains (Figure 3B). These results suggest that enhanced production of neurons upon impairment of $G\beta\gamma$ signaling in progenitors likely arose from increased neuronal differentiation of progenitor cells.

$G\beta\gamma$ Signaling Affects Cell-Fate Choices of Neural Progenitor Cells In Vitro

The increase in progenitors with a vertical cleavage plane (Figure 1) and the enhanced neuronal differentia-

tion of progenitors (Figures 2 and 3) upon disruption of $G\beta\gamma$ strongly argue that $G\beta\gamma$ signaling normally plays a regulatory role in the asymmetric division of progenitors. To test this hypothesis, we performed pair-cell analyses to closely follow the fate of the progeny of individual progenitor cells derived from control and β ARK-ct-expressing neocortices (Figure 4A). Briefly, dissociated progenitors from the anterior cortex were plated at clonal density and allowed to undergo one cell division in vitro. Pairs of GFP-positive cells generated by the division of GFP-labeled progenitor cells were fixed 20 hr after plating and analyzed by staining with the Tuj1 antibody. Consistent with the previous study (Shen et al., 2002), progenitor cells expressing the control GFP construct exhibited one of the three modes of cell division: P-P division—two daughter progenitor cells; P-N division—one daughter progenitor

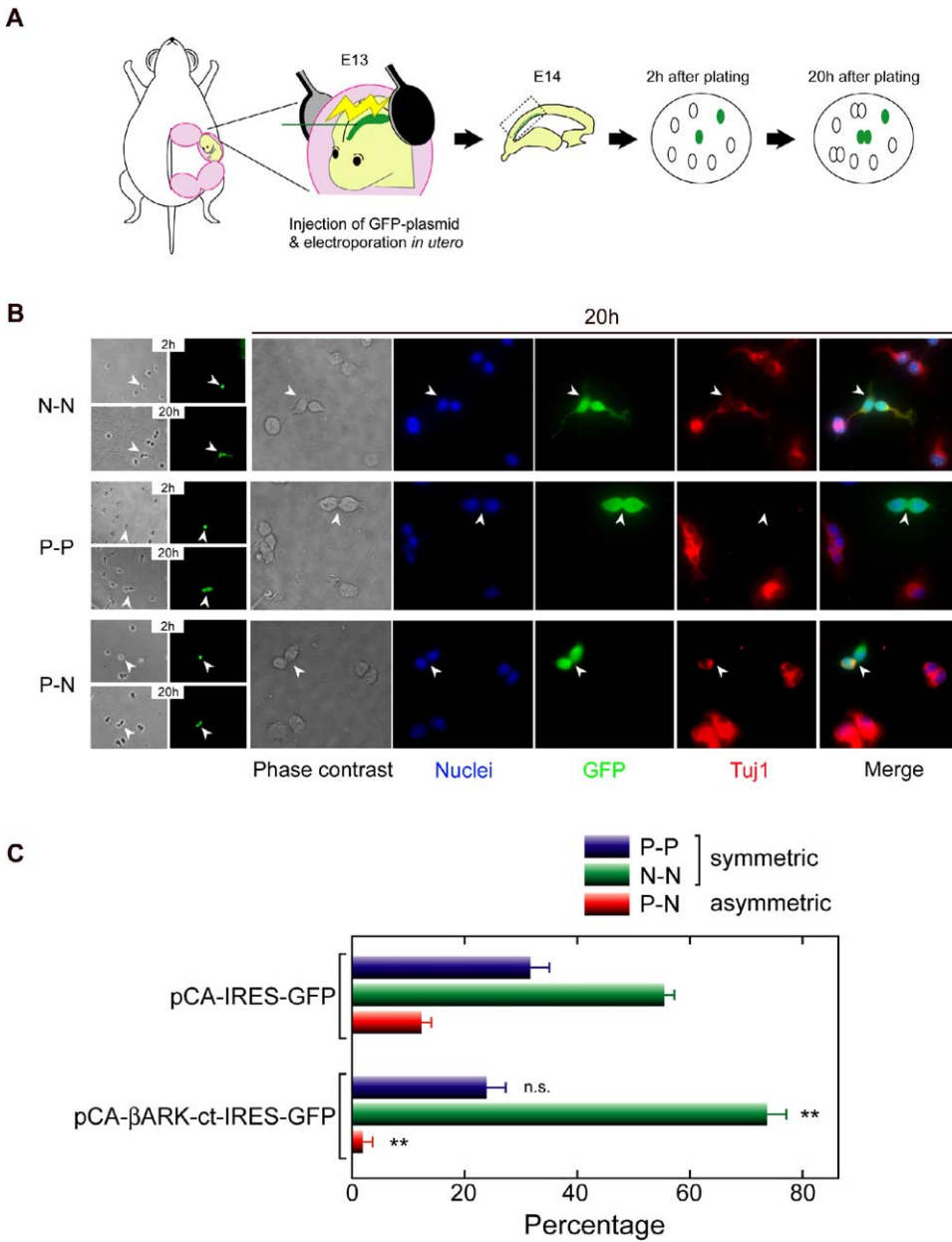


Figure 4. Mode of Cell Division Is Regulated by $G\beta\gamma$ Signaling

(A) The diagram illustrates the procedure for *in vitro* pair-cell analysis of gene-introduced progenitors (see text).

(B) Examples of three types of daughter-cell pairs generated from a single GFP-positive progenitor: two neurons (N-N, top panels), two progenitors (P-P, middle panels), and a progenitor and a neuron (P-N, bottom panels). Small panels on the left represent phase-contrast images (gray) and GFP images (green) of cortical cells 2 hr and 20 hr after plating. Similar fields of images obtained at each time point are shown. Single GFP-positive cells 2 hr after plating (arrowheads) divided and generated two GFP-positive daughter cells 20 hr after plating (arrowheads). The five panels on the right are high-magnification images of GFP-positive cells indicated by arrowheads in the small panels on the left (20 hr). Cultures were stained with antibodies against GFP (green) and Tuj1 (red). Nuclei were stained with Hoechst 33258 (blue).

(C) pCA-IRES-GFP or pCA- β ARK-ct-IRES-GFP was introduced into the neocortex, and pair-cell analysis was carried out. The percentage of P-P symmetric, N-N symmetric, and P-N asymmetric divisions was calculated and plotted as the mean \pm SEM ($n = 3$).

(Tuj1 negative) and one daughter neuron (Tuj1 positive); N-N division—two daughter neurons (Figure 4B). The proportion of N-N, P-N, and P-P divisions of the GFP-expressing progenitors was $55.7\% \pm 1.9\%$, $12.4\% \pm 1.7\%$, and $31.8\% \pm 1.8\%$, respectively ($n = 3$, 70 cells)

(Figure 4C). Progenitor cells expressing β ARK-ct showed a substantial decrease in asymmetric P-N division ($1.9\% \pm 1.9\%$, $n = 3$, 1 out of 61 cells) and a marked increase in N-N division ($74\% \pm 3.9\%$). These observations indicate that impaired $G\beta\gamma$ signaling in cortical

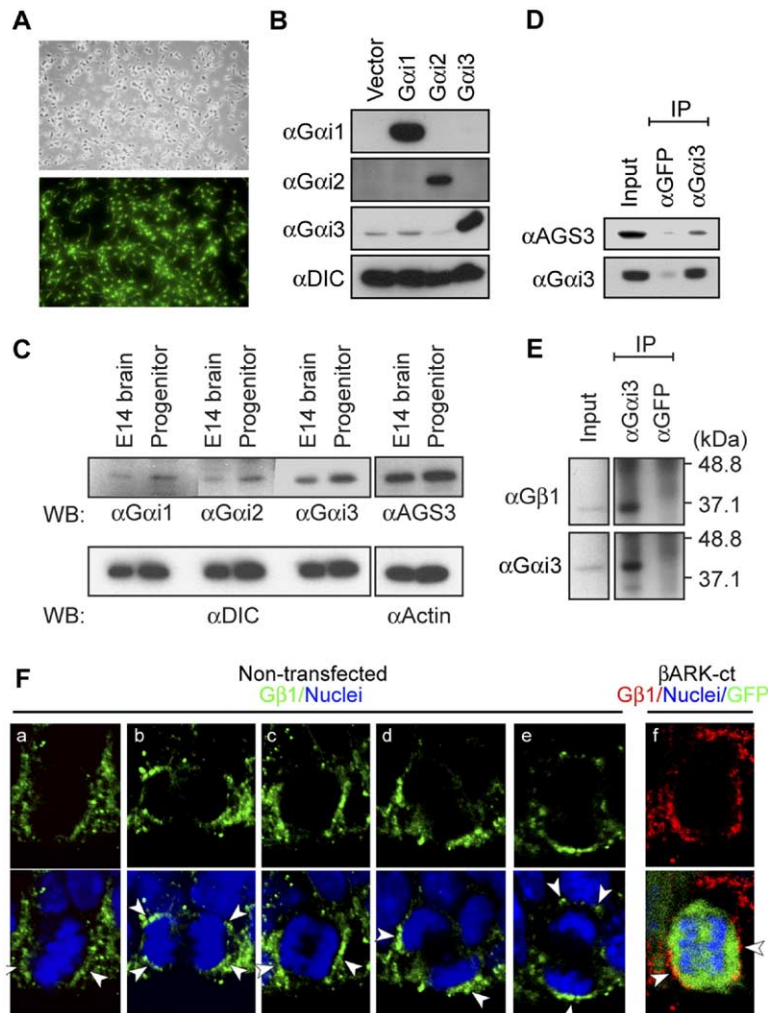


Figure 5. Interaction Between G α_i and AGS3 in Cultured Neural Progenitor Cells

(A) Neural progenitor cells cultured on dishes were stained with antibody against Nestin (top, phase-contrast image; bottom, Nestin immunoreactivity).

(B) HEK293T cells were transiently transfected with plasmids encoding mouse G α_i1 , G α_i2 , and G α_i3 . The cell lysates (10 μ g proteins) prepared 48 hr after transfection were immunoblotted with antibodies indicated. HEK293T cells express detectable level of endogenous G α_i3 .

(C) Cell lysates (10 μ g proteins) of cultured progenitor cells and E14 forebrain lysates (10 μ g proteins) were immunoblotted with antibodies against G α_i1 , G α_i2 , G α_i3 , dynein intermediate chain (DIC), and actin.

(D and E) Progenitor-cell extracts were immunoprecipitated with an anti-G α_i3 antibody, and the immunoprecipitates were immunoblotted with antibodies against AGS3 and G α_i3 (D) or antibodies against G β_1 and G α_i3 (E). Input in (D) is 1% of the starting material. In (E), immunoblots of input (2% of the starting material) (longer exposure) and immunoprecipitates (shorter exposure) are separately shown.

(Fa–Ff) Brain sections derived from E14 embryos were stained with anti-G β_1 antibody. Representative images of nontransfected dividing cells (Fa–Fe) and a pCA- β ARK-ct-IRES-GFP-transfected cell (Ff) are shown (a metaphase cell [Fa] and anaphase cells with various angles of the cleavage plane [Fb–Ff] are shown). G β_1 crescents are indicated by arrowheads.

progenitors results in overproduction of neurons as a consequence of both daughter cells adopting the neuronal fate.

AGS3 Associates with G α_i in the Neural Progenitor Cells

In *Drosophila* neuroblasts, a GPCR-independent activator of heterotrimeric G proteins, Pins, plays important roles in spindle positioning and orientation during asymmetric cell division. Mammalian AGS3 is an ortholog of *Drosophila* Pins. Functionally, AGS3 induces the dissociation of GDP bound G α_i from G $\beta\gamma$ by direct interaction with GDP bound G α_i , and the free G $\beta\gamma$ in turn activates downstream signaling events (Takesono et al., 1999; Natochin et al., 2000). We first determined whether AGS3 is expressed in the progenitor-cell population. In cultured progenitor cells (approximately 95% are Nestin positive, Figure 5A), AGS3, along with G α_i1 , G α_i2 , and G α_i3 , were all expressed (Figure 5C) as assessed by immunoblotting with antibodies specific to each G α_i subtype (Figure 5B). Importantly, G α_i3 antibody coimmunoprecipitated AGS3 in cultured progenitor cells (Figure 5D). Since antibodies against G α_i1 and

G α_i2 did not immunoprecipitate the respective G α_i proteins, the potential association of AGS3 with the other G α_i subtypes could not be determined. The physical interaction of AGS3 and G α_i3 suggests that these molecules likely function together in the progenitors to regulate the cleavage plane of their division.

Moreover, we found that the β_1 subunit of heterotrimeric G proteins (G β_1) was expressed in progenitors and associated with G α_i3 (Figure 5E). Importantly, localization of G β_1 in dividing progenitors correlated with the cleavage plane (Figures 5Fa–5Fe). In cells with the vertical cleavage plane, G β_1 immunoreactivity was prominent near the lateral or apical-lateral side of the cell cortex (Figures 5Fb and 5Fc), whereas in cells with the horizontal cleavage plane, G β_1 was localized to the apical and basal sides (Figure 5Fe). The G β_1 crescents were $81^\circ \pm 3^\circ$ from the axis of the cleavage plane ($n = 32$). Hence, the G β_1 crescents appeared to be approximately perpendicular to the cell-cleavage plane. In addition, overexpression of β ARK-ct did not seem to impact the subcellular distribution of G β_1 ($84^\circ \pm 4^\circ$ from the axis of the cleavage plane, $p > 0.6$, one-way ANOVA) (Figure 5Ff), which is consistent with the previ-

ous observation that β ARK is targeted to membrane bound $G\beta\gamma$, but does not extract $G\beta\gamma$ from the cell membrane (Pitcher et al., 1992). These observations lead to the notion that $G\beta 1/\gamma$ subunits establish the axis of division by localizing to the interface between astral microtubules and plasma membrane, thereby regulating their interactions.

Silencing of AGS3 Expression in Cortical Progenitors Causes Abnormalities Similar to Those Caused by Disruption of $G\beta\gamma$ Signaling

To examine whether AGS3 contributes to the regulation of spindle orientation and neurogenesis, we generated a DNA-based RNAi vector (Sui et al., 2002) to knock down the expression of AGS3. When the RNAi construct for AGS3 (pBS-U6-AGS3) was cotransfected with the GFP-tagged AGS3 in HEK293T cells (Figure 6A), the expression of AGS3 was substantially reduced as compared to the control plasmid (pBS-U6) and to the RNAi construct for $\alpha 3$ integrin (pBS-U6-VLA3; Sanada et al., 2004) ($p < 0.001$, $n = 4$, one-way ANOVA). We next introduced pBS-U6-AGS3 together with the GFP construct (pCA-IRES-GFP) into the VZ of E13 embryos and analyzed the orientation of cleavage planes at E15 (Figure 6B). As shown in Figure 6C, silencing of AGS3 expression caused an even more pronounced alteration in spindle orientation than that caused by β ARK-ct or $G\alpha i 3$ overexpression, with approximately 90% of GFP-positive progenitor cells displaying the vertical cleavage plane. This phenotype is consistent with the notion that AGS3 is an activator of $G\beta\gamma$ signaling, and silencing of AGS3 expression should lead to impairment of $G\beta\gamma$ signaling. Together with the observation that AGS3 directly associates with $G\alpha i 3$ in progenitors, these findings suggest that AGS3 regulates spindle orientation through activation of $G\beta\gamma$ in cortical progenitors.

To further investigate a role for AGS3 in regulating spindle orientation, we investigated whether there is a difference in the behavior of the metaphase plate in nontransfected and AGS3-silenced progenitor cells. As demonstrated in Figures 1A and 6D, nontransfected progenitor cells displayed dynamic rotation of the metaphase plate prior to chromosome separation. Conversely, when the AGS3 RNAi construct together with a DsRed2-expressing construct was introduced, the metaphase plate seemed to slightly seesaw along the apical-basal axis but failed to rotate during metaphase (Figures 6D and 6E), which is in agreement with the observation that the majority of AGS3-silenced progenitors displayed the vertical cleavage plane. Hence, these results reveal a critical role for AGS3- $G\beta\gamma$ signaling in the induction of metaphase rotation.

Spindle orientation is linked to cell polarity. To determine if polarity is disrupted by AGS3 knockdown or β ARK-ct overexpression, we utilized several well-characterized cell-polarity markers in progenitor cells (Chenn et al., 1998). We found that neither AGS3 knockdown nor overexpression of β ARK-ct affected the polarized structure of the progenitor cells, as judged by proper apical localization of pericentrin (a marker of centrioles), F-actin, and β -catenin (Figure S1). This suggests a direct and specific regulation of the mitotic spindle by the AGS3- $G\beta\gamma$ pathway. In addition, AGS3 RNAi did

not affect the apical localization of Numb (Zhong et al., 1996), a protein required for neuronal proliferation/differentiation during the mid-stages of neurogenesis (Li et al., 2003; Petersen et al., 2004). This suggests that alteration of cell-fate choices by impairing AGS3- $G\beta\gamma$ signaling is not linked to a change in Numb localization.

To further decipher a role for AGS3 on the cell-fate decision of neocortical progenitor cells, we analyzed the identities of AGS3-silenced cells. As shown in Figure 7A, the neuronal population (Tuj1 positive) in AGS3 RNAi plasmid-transfected neocortices was significantly increased ($70.9\% \pm 3.0\%$, $n = 3$) as compared to that in control plasmid-transfected cells ($53.3\% \pm 1.8\%$, $n = 3$, $p < 0.01$, one-way ANOVA). We then measured the mitotic index of AGS3 knockdown cells. In AGS3 RNAi electroporated neocortices, $1.0\% \pm 0.18\%$ ($n = 3$) of GFP-positive cells were positive for P-H3 (3 P-H3- and GFP-positive cells/326 GFP-positive cells located in the VZ), whereas $2.8\% \pm 0.11\%$ ($n = 3$) of GFP-positive cells were positive for P-H3 (9 P-H3- and GFP-positive cells/320 GFP-positive cells located in the VZ) in control GFP-electroporated neocortices (Figures 7B and 7D). This result underscores a significant reduction of the mitotic-cell fraction in AGS3-silenced brains. We further examined the cell-cycle-exit index of progenitors with silenced AGS3 expression. When the AGS3 RNAi construct was introduced (Figure 7C and 7D), we observed a close to 2-fold increase in the fraction of GFP-positive cells that exited the cell cycle as compared to those electroporated with the control GFP construct ($p < 0.05$, ANOVA). We also examined two other AGS3 RNAi constructs (pBS-U6-AGS3-2 and pBS-U6-AGS3-3) directed against a region different from that in pBS-U6-AGS3. The pBS-U6-AGS3-2 construct decreased GFP-tagged AGS3 expression to an extent comparable to pBS-U6-AGS3, whereas pBS-U6-AGS3-3 was less efficient (Figure S2). Cells introduced with pBS-U6-AGS3-2 showed phenotypes similar to those with pBS-U6-AGS3 in terms of spindle orientation, mitotic index, and cell-cycle-exit index (Figure S2). This result supports the observations made with pBS-U6-AGS3. Moreover, pBS-U6-AGS3-3, a less potent RNAi construct, had minor effects on spindle orientation, mitotic index, and cell-cycle-exit index, suggesting that a small amount of AGS3 is sufficient for normal regulation of spindle orientation and neurogenesis. Collectively, these observations suggest that disruption of $G\beta\gamma$ signaling by overexpression of β ARK-ct or $G\alpha i 3$, or by knocking down AGS3, results in the reorientation of mitotic spindles, alteration of cleavage planes, and exit from the cell cycle of neocortical progenitors.

Discussion

Role of $G\beta\gamma$ in Spindle Orientation and Cell-Fate Determination

In the developing ferret cerebral cortex, dividing progenitor cells with vertical cleavage planes give rise to daughter cells with similar developmental potentials (e.g., two progenitor cells) (Chenn and McConnell, 1995). In contrast, cell divisions with horizontal cleavage planes generate an apical daughter that remains a

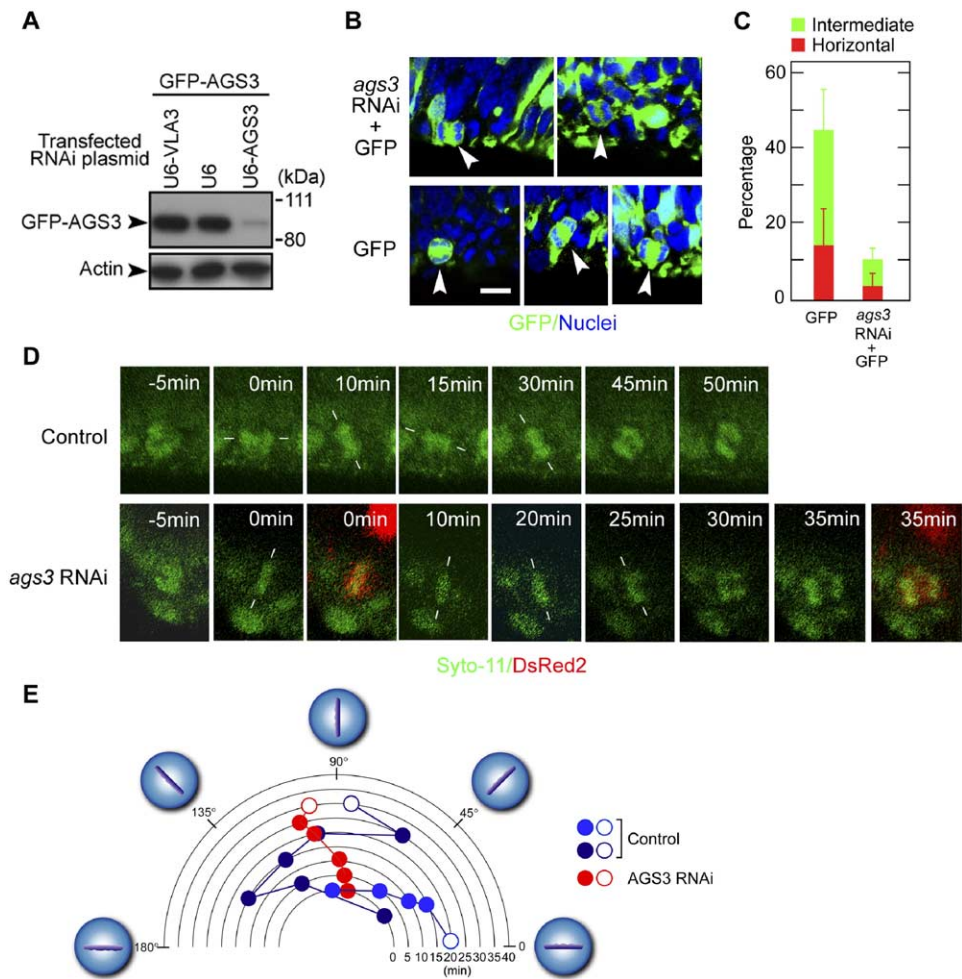


Figure 6. Knockdown of AGS3 Expression Results in Spindle-Orientation Abnormality

(A) HEK293T cells in 24-well plates were transiently transfected with various combinations of the GFP-tagged AGS3-expressing plasmid (GFP-AGS3, 0.1 μ g), α 3 integrin-RNAi plasmid (U6-VLA3, 1.0 μ g), control empty plasmid (U6, 1.0 μ g), and AGS3-RNAi plasmid (U6-AGS3, 1.0 μ g) as indicated. The cell lysates (10 μ g proteins) prepared 48 hr after transfection were immunoblotted with anti-GFP (top panel) and anti-actin (middle panel) antibodies.

(B and C) The pCA-IRES-GFP plasmid together with the U6-AGS3 RNAi plasmid was introduced into embryonic brains at E13. Brains were fixed at E15 and followed by immunohistochemistry with an anti-GFP antibody (green). Nuclei were stained with Hoechst 33258 (blue). Representative images of GFP-labeled dividing cells (arrowheads) are shown. Relative frequencies of cell divisions with vertical, intermediate (green), and horizontal (red) cleavage planes (B) were measured and plotted (C) as the mean \pm SEM ($n = 3-4$). Scale bar, 10 μ m.

(D) The pCA-DsRed2 plasmid together with the AGS3 RNAi plasmid was introduced into embryonic brains at E12.5. Cortical slices were prepared at E14 and labeled with Syto-11 (green). Thereafter, the modes of cell division of nontransfected (control, upper panels) and AGS3 knockdown cells (*ags3* RNAi, lower panels) in the VZ were analyzed. Time is denoted in the individual panels. The orientation of the long axis of the metaphase plate is marked by white lines. Time = 0 represents the time when the metaphase plate was initially identified after prophase (-5 min). Images of DsRed2 expression in the AGS3 knockdown cell were obtained at 0 min and 35 min.

(E) Angles of the metaphase plate at each time point were measured in relation to the ventricular surface and were plotted. Drawings surrounding the graph illustrate the appearance of metaphase plates with different orientations. The mode of divisions of two control cells and one AGS-silenced cell are shown. Open circles represent the orientation of the cleavage plane at the time of chromosome separation.

progenitor and a basal daughter that differentiates into a neuron. Similarly, progenitor cells in the rat retina (Cayouette and Raff, 2003) and mouse neocortex (Haydar et al., 2003) show a correlation of cell-cleavage orientation and cell fates. Based on these studies, orientation of cell divisions seems to be correlated with subsequent cell fates. To date, however, little is known about the molecular machinery that contributes to mitotic-spindle orientation in vertebrate neural progenitors during brain development.

In the present study, we demonstrate that *in vivo* disruption of the G $\beta\gamma$ signaling shifts the cell-cleavage plane from the horizontal to vertical orientation, which is accompanied by the adoption of both daughter cells to the neuronal fate and the loss of the progenitor population. Noticeably, the overproduction of neurons is not associated with an alteration of asymmetric localization of Numb *in vivo* (Figure S1) and in acutely dissociated cultured progenitors (Figure S3). Collectively, these findings demonstrate an important contribution

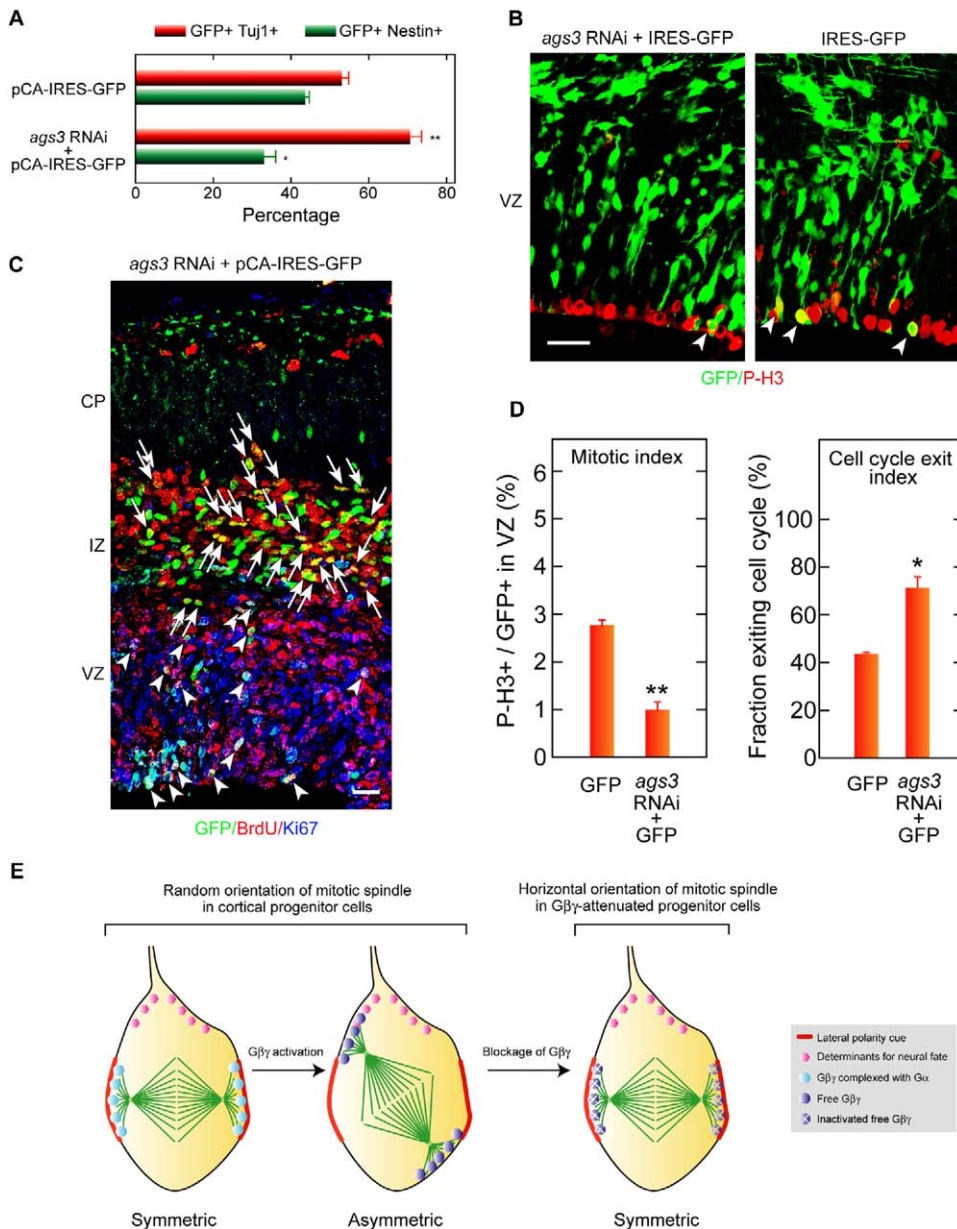


Figure 7. Silenced AGS3 Expression Induces Overproduction of Neurons through Enhanced Differentiation of Progenitor Cells.

(A) The pCA-IRES-GFP plasmid alone or together with the AGS3 RNAi plasmid was introduced into embryonic brains at E13, and 48 hr later, identities of GFP-positive cortical cells were examined as in Figure 2. * $p < 0.05$, ** $p < 0.01$ (one-way ANOVA).

(B) The pCA-IRES-GFP plasmid alone (right panel) or with the AGS3 RNAi plasmid (left panel) was introduced into embryonic brains at E13, and the brains were fixed at E15.

(C) The pCA-IRES-GFP plasmid with the AGS3 RNAi plasmid was introduced into embryonic brains at E13, BrdU was administered at E14, and the brains were fixed 24 hr after BrdU pulse labeling.

(D) The mitotic index was analyzed as in Figure 3A, and the cell-cycle-exit index was analyzed as in Figure 3B. Data are presented as the mean \pm SEM ($n = 3-4$). * $p < 0.05$, ** $p < 0.01$ (one-way ANOVA). Scale bars, 20 μ m.

(E) A model of Gβγ signaling in cortical progenitor cells. See Discussion.

of Gβγ signaling in regulating fate determination during cerebral cortical neurogenesis, which appears to be intimately linked to its role in regulating spindle orientation. We hypothesize that in neurogenic progenitor divisions, determinants for the neuronal fate might be asymmetrically localized at the basal side of the progenitor cells as described for *Drosophila* neuroblasts

(reviewed in Betschinger and Knoblich, 2004). In this scenario, when progenitors divide along the apical-basal axis, the determinants should exclusively segregate into the basal daughter cells and thereby induce asymmetric cell fates. On the other hand, progenitor divisions parallel to the ventricular surface lead to the partitioning of determinants into both daughters, and

thus two daughter neurons might be produced from a single progenitor cell. Indeed, this type of terminal neurogenic symmetric division is predicted to occur during the later stages of neurogenesis (Kornack and Rakic, 1995; Takahashi et al., 1996; Cai et al., 2002). Importantly, this model provides an explanation for why a shift of progenitor division along the apical-basal axis to planar axis upon G $\beta\gamma$ impairment leads to the hyperdifferentiation of progenitors and overproduction of neurons (Figure 7E). In support of this model, we demonstrate that normal neurogenic asymmetric cell divisions that generate one progenitor and one neuron are reduced by the disruption of G $\beta\gamma$ signaling, while terminal neurogenic symmetric divisions that produce two daughter neurons are increased as assessed by in vitro pair-cell analysis.

Recent studies show that a certain population of neural progenitors within the VZ produces one progenitor and one intermediate progenitor by asymmetric cell division. The intermediate progenitors in turn migrate to the basal region of the VZ (subventricular zone, SVZ) where they divide and predominantly generate two neurons (Miyata et al., 2004; Noctor et al., 2004). It is possible that impairment of G $\beta\gamma$ signaling results in the enhanced production of intermediate progenitors, eventually leading to overproduction of neurons. However, this model does not appear to be the case, as the ratio of dividing cells in the SVZ to those in the VZ did not increase but rather was significantly decreased in cortices expressing β ARK-ct or G α i3 (Figure S4). This result suggests that disruption of the G $\beta\gamma$ signaling affects two types of asymmetric cell divisions, namely, progenitor-neuron and progenitor-intermediate progenitor divisions, which in turn induces a shift from the asymmetric divisions to the neurogenic symmetric cell divisions by altering the orientation of spindles.

AGS3 as a Potential Regulator of G $\beta\gamma$ Signaling in Neural Progenitor Cells

Mammalian AGS3 has been shown to function as a guanine-nucleotide-dissociation inhibitor that binds to and stabilizes GDP bound G α i and thereby prevents GDP release (Natochin et al., 2000). Upon AGS3 binding to G α , G $\beta\gamma$ is released from GDP bound G α and in turn activates downstream signaling events (Takesono et al., 1999). We show that G α i3 associates with AGS3 in progenitors. Importantly, silencing of AGS3 affects the spindle orientation and cell-fate decisions of progenitor cells in a manner similar to attenuation of G $\beta\gamma$ signaling. Taken together, our findings illustrate a model by which G $\beta\gamma$ subunits are released from G α i upon association of AGS3 with G α i, leading to activation of G $\beta\gamma$ signaling. Furthermore, activated G $\beta\gamma$ is required for progenitor divisions along the apical-basal axis and proper cell-fate determination of progenitors.

Recently, an AGS3-related protein, mammalian Pins, has been shown to be required for dynamic microtubule instability by virtue of its association with G α i and NuMA, a microtubule binding protein (Du et al., 2001; Du and Macara, 2004). Interestingly, overexpression or silencing of Pins in MDCK cells disrupts NuMA localization and microtubule organization (Du et al., 2001). Unlike the changes observed upon silencing of Pins in

MDCK cells (Du et al., 2001), it is interesting to note that the pericentrosomal localization of NuMA, chromosome alignments, and chromosome segregation during mitosis did not seem to be affected by the silencing of AGS3 expression in neuronal progenitor cells (Figure S5). These observations suggest that AGS3 and Pins regulate microtubules through distinct pathways. Although the role of mammalian Pins in cortical progenitors remains to be elucidated, AGS3 and mammalian Pins may coordinately control the spindle orientation and dynamics of cortical progenitor cells.

Regulation of Mitotic-Spindle Orientation in Cerebral Cortical Progenitor Cells

In the mammalian neocortex, neural progenitor cells display various angles of spindle orientation during the peak of neurogenesis (Chenn and McConnell, 1995; Haydar et al., 2003; present study). By contrast, before the onset of neurogenesis and at later stages of neurogenesis, the majority of cells exhibit the vertical cleavage plane (Haydar et al., 2003). It has been hypothesized that symmetric cell division is regulated by a cue localized to the lateral cell cortex and recognized by the astral microtubules, causing the spindle to orient parallel to the ventricular surface (see Figure 7E). The masking or removal of the cue (or its recognition machinery) results in randomization of cleavage orientation, hence asymmetric cell division (Rhyu and Knoblich, 1995). Alternatively, it is also possible that asymmetric cell division is caused by the presence of another cue localized to the apical-basal axis that instructs the astral microtubules to orient the spindle perpendicular to the ventricular surface. In the present study, we demonstrate that attenuation of the G $\beta\gamma$ signaling markedly increases the vertical cleavage of progenitors. We hypothesized that when G $\beta\gamma$ signaling is inactive, the planar polarity cue directs the mitotic spindle to orient along the planar axis. On the other hand, the recognition of the planar polarity cue by astral microtubules is incapacitated upon activation of the G $\beta\gamma$ signaling, resulting in randomization of the spindle orientation (see Figure 7E). This model is in contrast to the roles of G proteins described in *Drosophila* neuroblasts and *C. elegans* embryos, in which G proteins are required either to connect astral microtubules to the cell cortex or to activate molecular motors that pull on the microtubules. Thereby, inactivation of G proteins results in randomization of the spindle orientation in these cells. In support of our model, the present study demonstrates that the metaphase plate did not show dynamic rotation upon silencing of AGS expression but rather was kept along the apical-basal axis. Furthermore, the G β 1 γ subunits in the progenitors localize to the cell cortex facing astral microtubules, supporting the idea that free G $\beta\gamma$ may attenuate the connection between astral microtubules and the polarity cue laterally located in progenitors. Alternatively, G $\beta\gamma$ may act on microtubules directly (Roychowdhury and Rasenick, 1997). Further identification of downstream effectors will help elucidate the mechanisms by which G $\beta\gamma$ controls the orientation of the mitotic spindle.

In conclusion, the present findings link a central process underlying cortical neurogenesis to the function

of heterotrimeric G proteins. The identification of important roles of G $\beta\gamma$ signaling in the regulation of spindle orientation and cell-fate choices of neural progenitor cells carries the hope of revealing new ways to decipher the complex events underlying neurogenesis in the developing neocortex.

Experimental Procedures

Preparation of Acute Brain Slices and Time-Lapse Image Acquisition

Brain slices were prepared as described previously (Sanada et al., 2004). The slices were incubated for 1 hr in culture media (neurobasal media [Invitrogen] supplemented with 1% penicillin-streptomycin, 1% glutamine, N2, and B27) containing 100 nM Syto-11 (Molecular Probes). Thereafter, the slices were destined for 30 min with culture media and overlaid with collagen on 35 mm dishes, followed by incubation with culture media for at least 30 min. The slices were then viewed at 37°C through a 63 \times (N.A. 0.95) Achromplan lens of the Zeiss LSM510 confocal system, and images were collected as image stacks of 6–8 z steps (approximately 5 μ m interval) every 5 min. The most superficial image of the z stack was approximately 100 μ m below the cut surface of the slice, and minimal laser throughput (approximately 4%) was used to ensure tissue viability during imaging.

Plasmids, In Utero Electroporation, and Immunohistochemistry

Plasmids used are described in the [Supplemental Experimental Procedures](#). In utero gene transfer by electroporation was performed as described previously (Sanada et al., 2004). Cryosections (20 μ m or 40 μ m) of brains were subjected to immunohistochemistry as described (Sanada et al., 2004). Primary antibodies used were anti-GFP polyclonal antibody (1:1000; Molecular Probes), anti-Nestin monoclonal antibody (Rat401, 1:500; BD Pharmingen), anti-pericentrin monoclonal antibody (1:200; BD Transduction Laboratories), anti- β -catenin monoclonal antibody (1:500; BD Transduction Laboratories), goat anti-Numb polyclonal antibody (1:100; Abcam), anti-G β 1 polyclonal antibody (1:100; Santa Cruz Biotechnology), and anti-NuMA antibody (Gaglio et al., 1995, 1:1000). Secondary antibodies used were fluorescein-conjugated goat anti-rabbit IgG antibody (1:400; ICN), Alexa568-conjugated goat anti-mouse IgG antibody (1:1000; Molecular Probes), and Alexa568-conjugated donkey anti-goat IgG antibody (1:1000; Molecular Probes). F-actin was visualized by rhodamine-phalloidin staining. The cell nuclei were stained with Hoechst 33258 (Sigma). Images were taken with a Zeiss LSM510 confocal microscope.

Quantification of the mitotic index and cell-cycle-exit index was performed as described in the [Supplemental Experimental Procedures](#).

For microtubule staining, brain slices (300 μ m) were prepared as described above. The slices were immediately fixed and staining was performed as described (Mandato and Bement, 2003).

Pair-Cell Analysis

Pair-cell analysis was performed according to Shen et al. (2002). Briefly, E13 embryos were electroporated with various genes together with GFP, and the dorsolateral cortices derived from the electroporated anterior telencephalons were dissected at E14, followed by careful removal of meninges. Thereafter, dispersed cortical cells were prepared (Shen et al., 2002) and plated at clonal density on wells of 60-well Terasaki plate (Grainer) in DMEM supplemented with 1% penicillin-streptomycin, 1% glutamine, N2, B27, and 10 ng/ml bFGF. GFP-labeled cells in each well were mapped 2 hr after plating to record their location, and the cultures were mapped again to identify daughter-cell pairs 20 hr after plating. Cells were then fixed and stained with anti-GFP polyclonal antibody and anti-Tuj1 antibody (1:500, Covance).

Cell Culture, Immunoprecipitation, and Immunoblotting

Cultures of cerebral cortical progenitor cells were prepared as described (Rajan and McKay, 1998). Immunoprecipitation and immu-

noblotting were performed as described in the [Supplemental Experimental Procedures](#).

Supplemental Data

Supplemental Data include Supplemental Experimental Procedures, Supplemental References, five figures, and one movie and can be found with this article online at <http://www.cell.com/cgi/content/full/122/1/119/DC1/>.

Acknowledgments

We thank Dr. R.J. Lefkowitz for the β ARK1 plasmid, Dr. T. Matsuda for the pCA-IRES-GFP and pCA-DsRed2 plasmids, Dr. Y. Shi for the pBS/U6 plasmid, and Dr. D. Compton for NuMA antibody. We are also grateful to C. Frank, B.A. Samuels, T. Shu, and D. Kim for critical reading of the manuscript and M. Ocana at the Harvard Center for Neurodegeneration and Repair for technical advice on confocal microscopy. K.S. is supported by the Uehara Memorial Foundation. This work was supported in part by NIH grants (NS37007) to L.-H.T. L.-H.T. is an investigator of the Howard Hughes Medical Institute.

Received: November 28, 2004

Revised: March 28, 2005

Accepted: May 6, 2005

Published: July 14, 2005

References

- Asano, T., Shinohara, H., Morishita, R., Ueda, H., Kawamura, N., Katoh-Semba, R., Kishikawa, M., and Kato, K. (2001). Selective localization of G protein γ 5 subunit in the subventricular zone of the lateral ventricle and rostral migratory stream of the adult rat brain. *J. Neurochem.* 79, 1129–1135.
- Betschinger, J., and Knoblich, J.A. (2004). Dare to be different: asymmetric cell division in *Drosophila*, *C. elegans* and vertebrates. *Curr. Biol.* 14, R674–R685.
- Cai, L., Hayes, N.L., Takahashi, T., Caviness, V.S., Jr., and Nowakowski, R.S. (2002). Size distribution of retrovirally marked lineages matches prediction from population measurements of cell cycle behavior. *J. Neurosci. Res.* 69, 731–744.
- Cayouette, M., and Raff, M. (2003). The orientation of cell division influences cell-fate choice in the developing mammalian retina. *Development* 130, 2329–2339.
- Chenn, A., and McConnell, S.K. (1995). Cleavage orientation and the asymmetric inheritance of Notch1 immunoreactivity in mammalian neurogenesis. *Cell* 82, 631–641.
- Chenn, A., and Walsh, C.A. (2002). Regulation of cerebral cortical size by control of cell cycle exit in neural precursors. *Science* 297, 365–369.
- Chenn, A., Zhang, Y.A., Chang, B.T., and McConnell, S.K. (1998). Intrinsic polarity of mammalian neuroepithelial cells. *Mol. Cell. Neurosci.* 11, 183–193.
- Cismowski, M.J., Takesono, A., Ma, C., Lizano, J.S., Xie, X., Fuemkranz, H., Lanier, S.M., and Duzic, E. (1999). Genetic screens in yeast to identify mammalian nonreceptor modulators of G-protein signaling. *Nat. Biotechnol.* 17, 878–883.
- Crespo, P., Xu, N., Simonds, W.F., and Gutkind, J.S. (1994). Ras-dependent activation of MAP kinase pathway mediated by G-protein $\beta\gamma$ subunits. *Nature* 369, 418–420.
- Du, Q., and Macara, I.G. (2004). Mammalian Pins is a conformational switch that links NuMA to heterotrimeric G proteins. *Cell* 119, 503–516.
- Du, Q., Stukenberg, P.T., and Macara, I.G. (2001). A mammalian Partner of inscuteable binds NuMA and regulates mitotic spindle organization. *Nat. Cell Biol.* 3, 1069–1075.
- Federman, A.D., Conklin, B.R., Schrader, K.A., Reed, R.R., and Bourne, H.R. (1992). Hormonal stimulation of adenyl cyclase through Gi-protein $\beta\gamma$ subunits. *Nature* 356, 159–161.

- Gaglio, T., Saredi, A., and Compton, D.A. (1995). NuMA is required for the organization of microtubules into aster-like mitotic arrays. *J. Cell Biol.* *131*, 693–708.
- Gilman, A.G. (1987). G proteins: transducers of receptor-generated signals. *Annu. Rev. Biochem.* *56*, 615–649.
- Gotta, M., Dong, Y., Peterson, Y.K., Lanier, S.M., and Ahringer, J. (2003). Asymmetrically distributed *C. elegans* homologs of AGS3/PINS control spindle position in the early embryo. *Curr. Biol.* *13*, 1029–1037.
- Haydar, T.F., Ang, E., Jr., and Rakic, P. (2003). Mitotic spindle rotation and mode of cell division in the developing telencephalon. *Proc. Natl. Acad. Sci. USA* *100*, 2890–2895.
- Koch, W.J., Hawes, B.E., Inglese, J., Luttrell, L.M., and Lefkowitz, R.J. (1994). Cellular expression of the carboxyl terminus of a G protein-coupled receptor kinase attenuates G $\beta\gamma$ -mediated signaling. *J. Biol. Chem.* *269*, 6193–6197.
- Kornack, D.R., and Rakic, P. (1995). Radial and horizontal deployment of clonally related cells in the primate neocortex: relationship to distinct mitotic lineages. *Neuron* *15*, 311–321.
- Li, H.S., Wang, D., Shen, Q., Schonemann, M.D., Gorski, J.A., Jones, K.R., Temple, S., and Jan, N.Y. (2003). Inactivation of Numb and Numlike in embryonic dorsal forebrain impairs neurogenesis and disrupts cortical morphogenesis. *Neuron* *40*, 1105–1118.
- Mandato, C.A., and Bement, W.M. (2003). Actomyosin transports microtubules and microtubules control actomyosin recruitment during *Xenopus* oocyte wound healing. *Curr. Biol.* *13*, 1096–1105.
- Miyata, T., Kawaguchi, A., Okano, H., and Ogawa, M. (2001). Asymmetric inheritance of radial glial fibers by cortical neurons. *Neuron* *31*, 727–741.
- Miyata, T., Kawaguchi, A., Saito, K., Kawano, M., Muto, T., and Ogawa, M. (2004). Asymmetric production of surface-dividing and non-surface-dividing cortical progenitor cells. *Development* *131*, 3133–3145.
- Mochizuki, N., Cho, G., Wen, B., and Insel, P.A. (1996). Identification and cDNA cloning of a novel human mosaic protein, LGN, based on interaction with G α i2. *Gene* *181*, 39–43.
- Natochin, M., Lester, B., Peterson, Y.K., Bernard, M.L., Lanier, S.M., and Artemyev, N.O. (2000). AGS3 inhibits GDP dissociation from G α subunits of the Gi family and rhodopsin-dependent activation of transducin. *J. Biol. Chem.* *275*, 40981–40985.
- Noctor, S.C., Flint, A.C., Weissman, T.A., Dammerman, R.S., and Kriegstein, A.R. (2001). Neurons derived from radial glial cells establish radial units in neocortex. *Nature* *409*, 714–720.
- Noctor, S.C., Martinez-Cerdeno, V., Ivic, L., and Kriegstein, A.R. (2004). Cortical neurons arise in symmetric and asymmetric division zones and migrate through specific phases. *Nat. Neurosci.* *7*, 136–144.
- Petersen, P.H., Zou, K., Krauss, S., and Zhong, W. (2004). Continuing role for mouse Numb and Numbl in maintaining progenitor cells during cortical neurogenesis. *Nat. Neurosci.* *7*, 803–811.
- Pitcher, J.A., Inglese, J., Higgins, J.B., Arriza, J.L., Casey, P.J., Kim, C., Benovic, J.L., Kwatra, M.M., Caron, M.G., and Lefkowitz, R.J. (1992). Role of $\beta\gamma$ subunits of G proteins in targeting the β -adrenergic receptor kinase to membrane-bound receptors. *Science* *257*, 1264–1267.
- Rajan, P., and McKay, R.D. (1998). Multiple routes to astrocytic differentiation in the CNS. *J. Neurosci.* *18*, 3620–3629.
- Rhyu, M.S., and Knoblich, J.A. (1995). Spindle orientation and asymmetric cell fate. *Cell* *82*, 523–526.
- Roychowdhury, S., and Rasenick, M.M. (1997). G protein $\beta 1\gamma 2$ subunits promote microtubule assembly. *J. Biol. Chem.* *272*, 31576–31581.
- Sanada, K., Gupta, A., and Tsai, L.H. (2004). Disabled-1-regulated adhesion of migrating neurons to radial glial fiber contributes to neuronal positioning during early corticogenesis. *Neuron* *42*, 197–211.
- Schaefer, M., Petronczki, M., Dorner, D., Forte, M., and Knoblich, J.A. (2001). Heterotrimeric G proteins direct two modes of asymmetric cell division in the *Drosophila* nervous system. *Cell* *107*, 183–194.
- Shen, Q., Zhong, W., Jan, Y.N., and Temple, S. (2002). Asymmetric Numb distribution is critical for asymmetric cell division of mouse cerebral cortical stem cells and neuroblasts. *Development* *129*, 4843–4853.
- Shinohara, H., Udagawa, J., Morishita, R., Ueda, H., Otani, H., Semba, R., Kato, K., and Asano, T. (2004). Gi2 signaling enhances proliferation of neural progenitor cells in the developing brain. *J. Biol. Chem.* *279*, 41141–41148.
- Sui, G., Soohoo, C., Affar, E.B., Gay, F., Shi, Y., Forrester, W.C., and Shi, Y. (2002). A DNA vector-based RNAi technology to suppress gene expression in mammalian cells. *Proc. Natl. Acad. Sci. USA* *99*, 5515–5520.
- Takahashi, T., Nowakowski, R.S., and Caviness, V.S., Jr. (1996). The leaving or Q fraction of the murine cerebral proliferative epithelium: a general model of neocortical neuronogenesis. *J. Neurosci.* *16*, 6183–6196.
- Takesono, A., Cismowski, M.J., Ribas, C., Bernard, M., Chung, P., Hazard, S., 3rd, Duzic, E., and Lanier, S.M. (1999). Receptor-independent activators of heterotrimeric G-protein signaling pathways. *J. Biol. Chem.* *274*, 33202–33205.
- Zhong, W., Feder, J.N., Jiang, M.M., Jan, L.Y., and Jan, Y.N. (1996). Asymmetric localization of a mammalian Numb homolog during mouse cortical neurogenesis. *Neuron* *17*, 45–53.